P7.22 FORMULATION OF A SUITE OF RETRIEVAL ALGORITHMS FOR THE RETRIEVAL OF CIRRUS MICROPHYSICAL PROPERTIES USING RADAR, LIDAR AND RADIOMETER OBSERVATIONS APPLICABLE TO SATELLITE, AIRBORNE AND GROUND-BASED PLATFORMS

Yuying Zhang [a,*] Gerald G. Mace [a], G. M. Heymsfield [b], M. McGill [b], L. Avallone [c], E. Weinstock [d], S. Platnick [b], P. Yang [e]
[a] Department of Meteorology, University of Utah [b] NASA Goddard Space Flight Center
[c] Colorado University [d] Harvard University [e] Texas A&M University

1. INTRODUCTION

Cirrus clouds have an annual global and local frequency of occurrence of about 30% (i.e., Mace et al. 1997; Mace et al. 2001; Wylie et al. 1989; Wylie et al. 1994; Rossow and Schiffer 1999). As such, Cirrus clouds have a critical and complicated impact on the radiation balance of the Earth-atmosphere system because these clouds reflect incoming solar radiation and absorb and emit longwave radiation in amounts that depend on widely varying cloud layer properties. The relative magnitudes of the net radiative effects and their spatial and temporal variability, which is poorly represented in GCMs, depend on the cloud macroscale and microphysical properties. Inadequate knowledge of the distribution of cirrus cloud properties on a global scale limits our ability to determine either the sign or the magnitude of their net radiative impact (Stephens et al. 1990; Cess et al. 1996). A consistent validated global description of cloud properties is required in order to bridge the gap between models and observations.

The NASA ESE has a leading role in creating such datasets through its EOS program. The flagship satellites, Terra, Aqua, and Aura, have been launched. The moderate resolution Spectroradiometer (MODIS; King et al. 2003), is a cross-track multispectral-imaging instrument flown on Terra and Aqua. MODIS is a passive radiometer, and observes scattered and emitted upwelling reflectance and radiance from the surface and atmosphere. In April 2005, the first active remote sensors designed for probing the microphysical properties of clouds will be launched. CloudSat (a millimeter-wave radar) and CALIPSO (an optical lidar) will be inserted into an orbit nearly identical to that of Aqua. The two remote sensors observe vertical profiles of backscattered power at different wavelengths. Cloud height information can be obtained based on the vertical profiles from the active sensors. The constellation of satellites will be referred to as the A-Train. The footprints of MODIS, CloudSat and Calipso will often overlap each other within 1 minute.

The A-Train provides many opportunities to obtain a global dataset of cirrus properties that will improve our current understanding of cirrus. Much of our current global perspective derives from spectral radiances measured by sensors on satellites. Combining the observations of the different sensors in the A-Train is a key aspect of the observing philosophy. The observations from these sensors, when combined, provide rich sources of information for evaluating cloud properties, and the information from different sensors. Since the observations do not necessarily provide directly with useful information, cloud property retrieval algorithms are needed to convert the data streams from radiance, lidar backscatter, and radar reflectivity into cirrus properties of interest. In this paper, we describe the development of a suite of retrieval algorithms that will derive cloud microphysical and optical properties from A-Train satellite data.

* Corresponding author address: Yuying Zhang, Dept. Meteorology, Univ. of Utah, SLC UT84112-0110; Email: zyuying@met.utah.edu

2. DESCRIPTION OF RETRIEVAL ALGORITHMS

A millimeter radar observes backscattered energy that is weighted to the large particles in the crystal size distribution. The Lidar signal is backscattered energy that is weighted more toward the small particles but cannot penetrate thick clouds. A radiometer measures an integral radiance that emanates from the entire layer. Our goal is to exploit the strengths of each of these measurement strategies to create a reasonable description of the cloud microphysical properties.

Table 1 is a schematic of the algorithm suite we are developing to retrieve the layer-mean properties of optically thin cirrus: each row of the table represents a specific algorithm for retrieving layer-mean cloud properties. The forward model is based on some set of simplifying assumptions that describe the measurement in terms of the cloud properties. Since the description of particle size distribution requires at least 2 free parameters, two reasonably independent measurements must be used to characterize the cloud properties. The first three rows are the combinations of any arbitrary two observations from the three. By assuming an exponential size distribution, cloud properties can be retrieved. If we combine three observations, we can assume a fully defined gamma size distribution which more generally describes the size distribution. Also, other combinations of data are possible. For example, for each of the algorithms we

Observations			assumption
Radar	Lidar	Radiometer	
Z	T (β_{ext})	ε (β_{abs})	
X	X		$n(L) = n_e \exp(-\lambda_e L)$
X		X	
	X	X	
X	X	X	$n(L) = n_m (\frac{L}{L_m})^{\alpha} e^{\alpha} \exp(\frac{\alpha L}{L_m})$

Table 1. A suite of retrieval algorithms with different combinations of observations

can use lidar and radar profiles to retrieve cloud vertical structure with appropriate assumptions.

In order to avoid errors associated with the underlying atmosphere, we use a CO2 channel (Wylie and Menzel 1989; Wylie et al. 1994) to convert the cloud layer radiance into a measurement of emissivity. Since this is a thermal infrared radiance, we can derive the cloud emissivity during nighttime as well as daytime. The cloud emissivity is derived from a calculation of radiative transfer. If we assume overcast cirrus is observed in the FOV, we have this equation:

$$\varepsilon = \frac{R(\lambda) - R_{clr}(\lambda)}{B[\lambda, T_c] - R_{clr}(\lambda)} \quad (1)$$

where R(λ) is the observed cloudy-sky radiance, $R_{clr}(\lambda)$ is the clear-sky radiance calculated based on atmospheric profile, B[λ,Tc] is the Plank function at cloud top temperature. To determine cloud layer visible transmissivity, we use lidar signals in two independent vertical windows. When the lidar signals are fitted well, we can derive transmissivity (Mitrescu and Stephens 2002; Young 1995).

In order to retrieve cloud properties, the layer-mean ice crystal size spectrum is assumed in the form of a two-parameter zeroth order gamma (exponential) function $n(L)=N_e\exp(-\lambda_e L)$, where L is the maximum dimension of the nonspherical ice crystal, N_e is the number per unit length per unit volume of particles and λ_e is the logarithmic slope of the size spectrum and has units of inverse length. The infrared absorption coefficient ($\beta_{abs} = \int_0^\infty Q_{abs}(L)A(L)n(L)dL$) is derived from cloud emissivity ($\varepsilon = 1 - \exp[-\beta_{abs}\Delta h]$). Q_{abs} is calculated by Dr. Ping Yang (2004) based on a composite method using T_matrix, GOM, and Mie theory. Q_{ext} is the visible extinction coefficient ($\beta_{ext} = \int_0^\infty Q_{ext}A(L)n(L)dL$) derived from cloud transmissivity and is assumed to be a constant (2). Since ice crystals are not solid spheres, the forward model is built on some set of empirical relations that relate, respectively, the cross sectional area, the radar reflectivity and the mass of an individual particle to its maximum dimension (*L*):

$$\begin{aligned} A(L) &= a_A L^{bA} \\ dZ(L) &= a_z L^{bz} \\ m(L) &= a_m L^{bm} \end{aligned} \quad (2)$$

The algorithms are formulated and solved in an optimal estimation framework (Rodgers (1976, 2000)) that allows us to objectively determine error and track sources of uncertainty.

3. SENSITIVITY STUDY

The sensitivities of retrieved IWP to the observations for the radar-lidar combinations are shown in Figure 1 by assuming a 1-km thin cirrus, and the sensitivity for mass mean length in Figure 2. For the combination of radiometer and lidar, since both measurements are related to the 2nd moment of the particle size distribution , the information in the data reduces to differences in the ratio of the infrared Q_a and visible Q_e as a function of particle size. All retrieved values lie close along the diagonal. A slight change in observations will cause large bias of the retrieved values. Clearly the lidar/radiometer algorithm this is the most unstable algorithm of the three. Figure 3 makes this tendency clearer.

Also, the retrieved properties are very sensitive to the empirical constants. For example, for the combination of radar and lidar (Figure 4), when a_m decreases and increases 50 percent, IWC changes linearly, but nonlinearly with a_a and a_z. IWC is quite sensitive to the specified values of b_m, b_a and b_z. From the sensitivity analysis of cloud properties to the empirical constants, we can also see the large uncertainties that derive from the small uncertainties in the empirical constants.

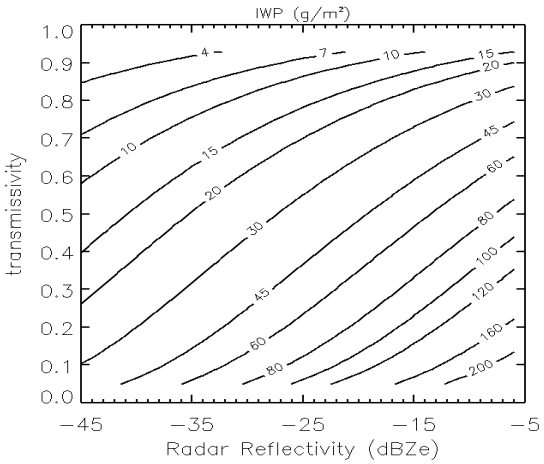

Figure 1. Sensitivity of IWP to observations for the lidar-radar combination.

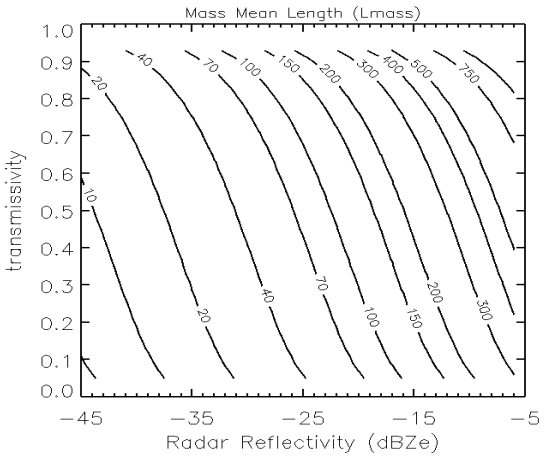

Figure 2. Sensitivity of Lmass to observations for the lidar-radar combination.

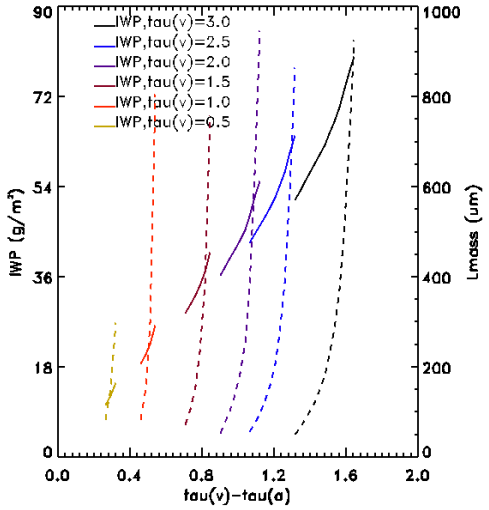

Figure 3. Sensitivities of IWP and Lmass to the difference between visible optical depth and infrared optical depth.

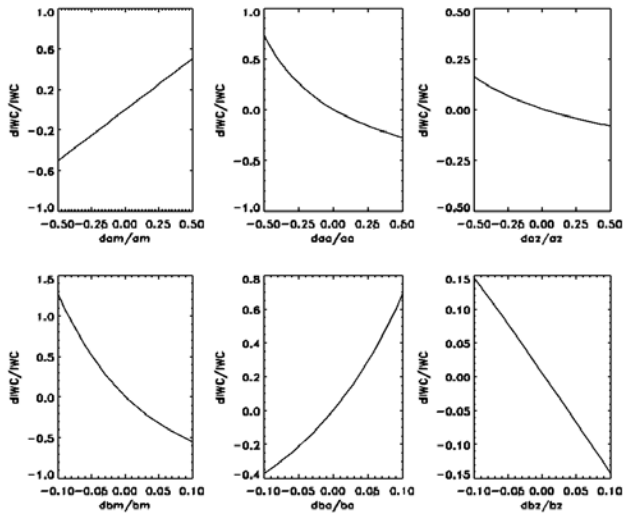

Figure 4. Sensitivities of IWC to empirical constants for the combination of radar and lidar.

4. IMPLEMENTATION

Prior to the launch of the satellites carrying active sensors, the implementation of the algorithms currently being developed can be performed using data collected in field programs. The CRYSTAL-FACE mission in July 2002 provides detailed measurements of clouds, and will help us investigate the properties of tropical cirrus clouds. The ER2 is one of the six aircrafts equipped with state-of-the-art instruments, and flew at 65,000 feet (20km) above Florida during the CRYSTAL-FACE mission. Based on the aircraft altitude, the instruments on the ER2 are able to observe 94% of the earth's atmosphere, thus the ER2 instruments function as spaceborne instrument simulators.

On July 26 2002, two aircraft, the ER2 and WB57, flew southbound, turned around, and then flew northbound during the time period 18:06:00 to 19:12:00 (UTC) hours. This extensive cirrus event is representative of tropical cirrus. Figure 5 (a) is a visible image created by combining 3 visible channels and figure 5 (b) is a CO2 channel image. Both figures show data observed by MODIS on Aqua, and the aircraft's flight tracks are plotted on both images. Circle 1 shows convection; circle 2 shows cirrus; and circle 3 shows low layer cloud. In the CO2 channel figure, circle 3 is empty because lower cloud is 'hidden' by the absorption in the CO2 channel. Figure 6 shows the lidar signal, radar reflectivity, brightness temperature, and retrieved layer-mean IWC for the southbound leg in (a) and northbound leg in (b). Radar cannot see most of the cloud layer because small particles dominate in those areas. When retrieved IWC reaches its peaks, Tb decreases and radar detects part of the cloud layer. Convection occurred from 18.5 to 18.6 (UTC) hours, and an anvil at 18.83 (UTC) hours possibly separated from the top of the convection.

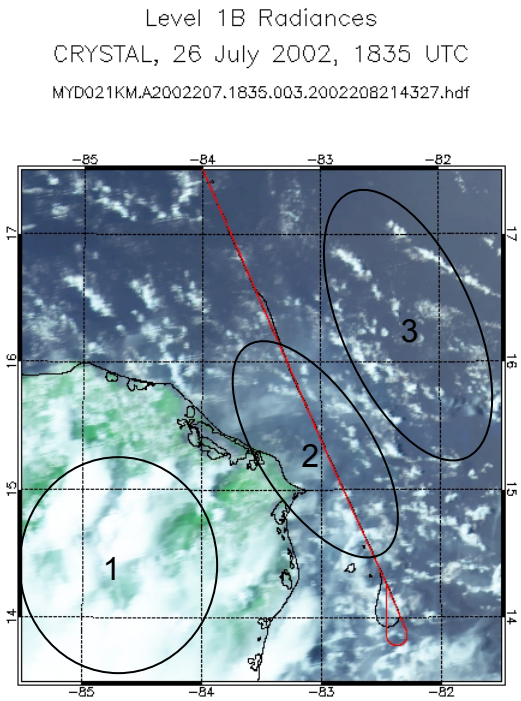

Figure 5. (a) visible channels observed by MODIS on Aqua, ER2 aircraft flight track in red, and WB57 aircraft flight track in black.

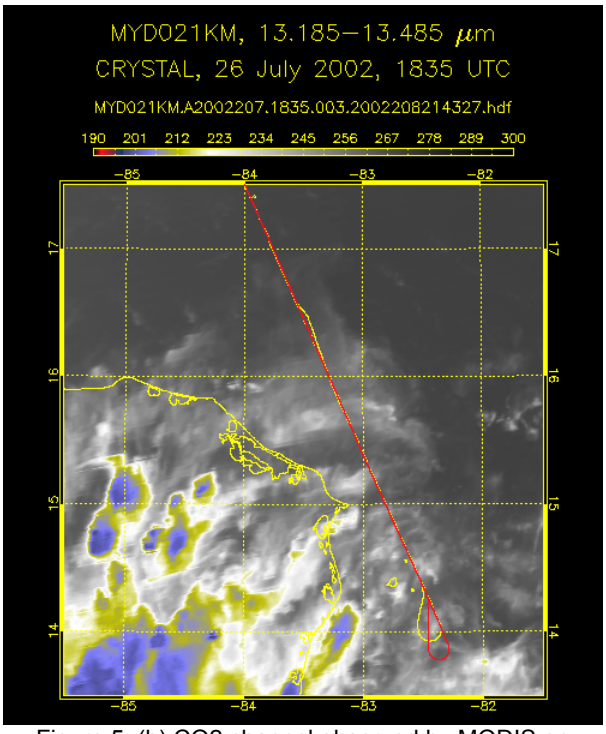

Figure 5. (b) CO2 channel observed by MODIS on Aqua, ER2 aircraft flight track in red, and WB57 aircraft flight track in yellow.

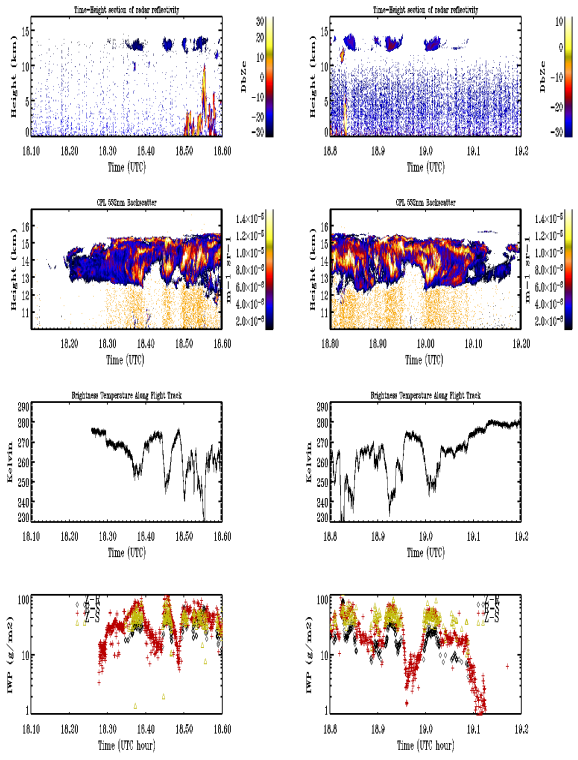

Figure 6. (a)southbound leg and (b)northbound leg, CRS, CPL, Tb, and retrieved IWC.

The WB57 penetrated the cloud layer at around 19 UTC hours, and the aircraft flight track is illustrated together with the ER2 observations in figure 7 in which a temporal offset is added based on the calculation of the spatial match for the two aircraft. Figure 8(a) is the particle sample collected by the CPI on the WB57, and shows concentrated small ice crystals. So for these ice crystals, b_m is close to 3 and b_a is close to 2, which are close to the coefficients for spherical particles. The overlap of the ER2 and WB57 flight tracks is depicted in figure 8(b). The retrieved layer-mean IWC is plotted together with in situ measurements in figure 7(d). After 19 (UTC) hours, the Harvard data (Weinstock et al. 1994) falls within our 1 sigma uncertainty but the CU data falls outside of this uncertainty, and that it is unclear which measure of IWC is most reasonable in this case. The retrieved IWC is much larger than in situ data before 19 (UTC) hours because the WB57 only flew through the upper layer, and most of the large particles are concentrated below. This structure is shown in the radar reflectivity (figure 7(a)). The high retrieved IWC is proven by the decrease in MAS brightness temperature, and is indicated by the green circle in figure 8(b).

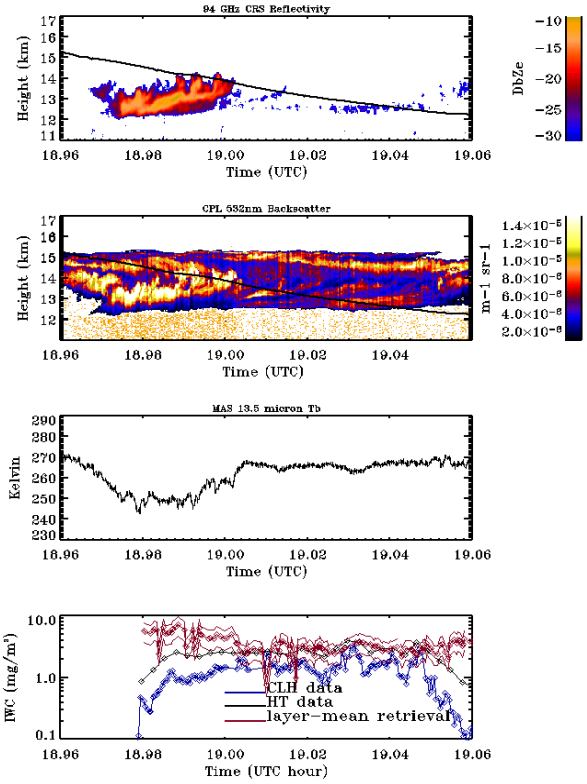

Figure 7. WB57 aircraft flight track plotted together with ER2 radar and lidar observations, and retrieved layer-mean IWC compared with in situ data (CLH data provided by L. Avalone, Colorado University; HT data provided by E. Weinstock, Harvard University)

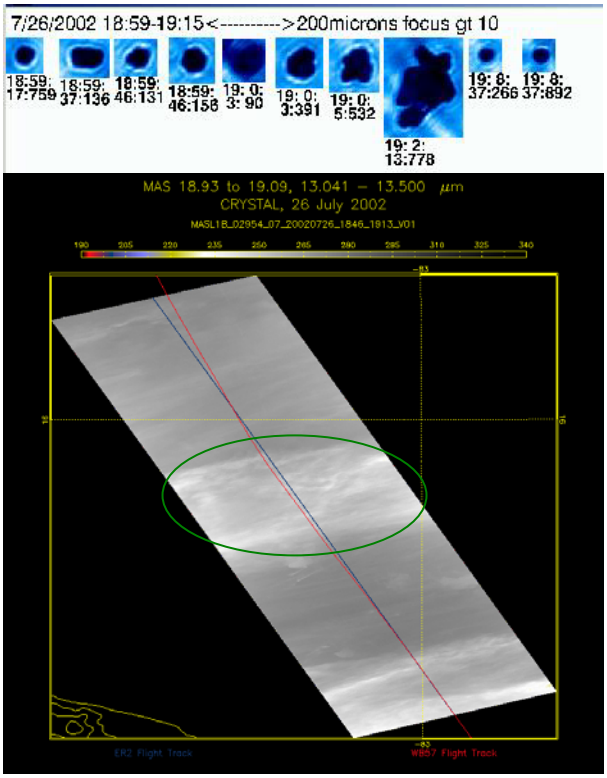

Figure 8. (a) particle samples collected by CPI on WB57, (b) WB57 and ER2 flight tracks overlapped on MAS observation.

MODIS on Aqua overpassed the CRYSTAL-FACE site at 18.6 UTC hours. We track the MODIS data forward and backward based on the ER2 aircraft position for a total of 40 minutes, and the comparisons are shown in figure 9. Unfortunately, there is convection below at the overpass time, but the fitted structures can be seen in the two far wings. The large IWC and optical depth come from convection, since the MOD06 cloud products are retrieved with the assumption of single layer cloud. In the comparison of frequency distributions for small values, the MOD06 retrieved IWC is still biased high, while the optical depths agree well.

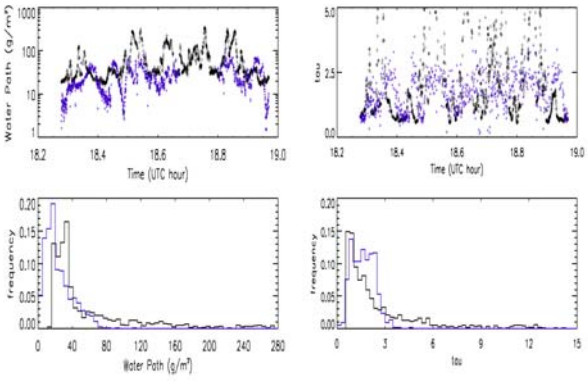

Figure 9. retrieved IWP and optical depth compared with MOD06 cloud products as both value comparison and frequency distribution comparison.

5. DISCUSSION

In this paper, we describe a suite of cloud property retrieval algorithms designed to treat thin cirrus observed by lidar, mm radar and radiometer that uses an optimal estimation theory inversion framework. The algorithms, in their current formulation, assume an exponential distribution of ice crystals and retrieve layer mean properties. Our goal is to implement this suite of algorithms using the A-Train data streams that include the Cloudsat radar, Calipso lidar and Aqua MODIS observations. In this paper the lidar-radiometer algorithm is implemented using data collected in thin cirrus during the Crystal FACE field campaign collected during a survey flight that penetrated into the tropical waters east of the Yucatan Peninsula. Comparing the retrieved IWC with data collected by water content probes on the WB57, the lidar-radiometer algorithm produces reasonable values. From the sensitivity study, the empirical constants that relate mass and area to particle maximum dimension are critical to the algorithm accuracy. Since our goal is to process global data, more in situ data are needed to constrain these empirical relationships.

REFERENCES:

Aydin, Kultegin and Thomas M. Walsh, 1999: Millimeter wave scattering from spatial and planar bullet rosettes. IEEE Transactions on Geoscience and Remote Sensing, 37, 1138-1150.

Cess, R. D., et al., 1996: Cloud feedback in atmospheric general circulation models: an update. J. Geophy. Res., 101, 12791-12794.

Dowling, D. R., and L. F. Radke, A summary of the physical properties of cirrus clouds, *J. Appl. Meteorol.*, 29, 970-978, 1990.

Heymsfield, Andrew J. and Jean Iaquinta, 2000: Cirrus crystal terminal velocities. J. Atmos. Sci., 57, 916-942.

Liou, K. N., 1986: Influence of cirrus clouds on weather and climate processes: a global perspective. *Mon. Wea, Rev.*, 114, 1167-1199.

Mace, G. G., T. P. Ackerman, and E. E. Clothiaux, 1997: A study of composite cirrus morphology using data from a 94-GHz radar and correlations with temperature and large-scale vertical motion. *J. Geo. Res.*, 102(D12), 13,581-13,593.

Mace, G. G., E. E. Clothiaux, and T. A. Ackerman, 2001: The composite characteristics of cirrus clouds: bulk properties revealed by one year of continuous cloud radar data. *J. Climate*, 14, 2185-2203.

Mitchell, D. L., 1996: Use of Mass- and Area-Dimensional Power Laws for determining precipitation particle terminal velocities. *J. Atmos. Sci.*, 53, 1710-1723.

Mitrescu, C. and G. L. Stephens, 2002: A new method for determining cloud transmittance and optical

depth using the ARM micropulsed lidar. J. Atmos. & Oceanic Tech., 19, 1073-1081.

Stephens, G. L., S.-C. Tsay, J. P. W. Stackhouse, and P. J. Flatau, 1990: the relevance of the microphysical and radiative properties of cirrus clouds to climate and climatic feedback. *J. Atmos. Sci.*, 47, 1742-1753.

Rodgers, C. D., 1976: Retrieval of atmospheric temperature and composition from remote measurements of thermal radiation. Rev. Geophys. Space. Phys., 14, 609-624.

Rodgers, C. D., 2000: Inverse Methods for Atmospheric Sounding : Theory and Practice (Series on Atmospheric Oceanic and Planetary Physics). World Scientific.

Rossow, W. B., and R. A. Schiffer, 1999: Advances in understanding clouds from ISCCP. *Bull. Amer. Metero. Soc.*, 80, 2261-2286.

Yang, Ping, M. G. Mlynczak, H.L. Wei, D. P. Kratz, B,A. Baum , Y. X. Hu, W. J. Wiscombe, A. Heidinger, and M. I. Mishchenko, 2003: Spectral signature of cirrus clouds in the far-infrared region: single-scattering calculation and radiative sensitivity study. J. Geophys. Res. 108(D18),4569.

Young, Stuart A., 1995: Analysis of lidar backscatter profiles in optically thin clouds. Applied optics, 30, 7019-7031.

Weinstock, E. M., et al., 1994: New fast response photofragment fluorescence hygrometer for use on the NASA ER-2 and the Perseus remotely piloted aircraft, Rev. Sci. Instrum. 65, 3544-3554.

Wylie, D.P., and W.P. Menzel, 1989: Two years of cloud cover statistics using VAS. J. Climate Appl. Meteor., 2, 380-392.

Wylie, D.P., Menzel, W.P., Woolf, H.M., and Strabala, K.I., 1994: Four years of global cirrus cloud statistics using HIRS. J. Climate, 7, 1972-1986.